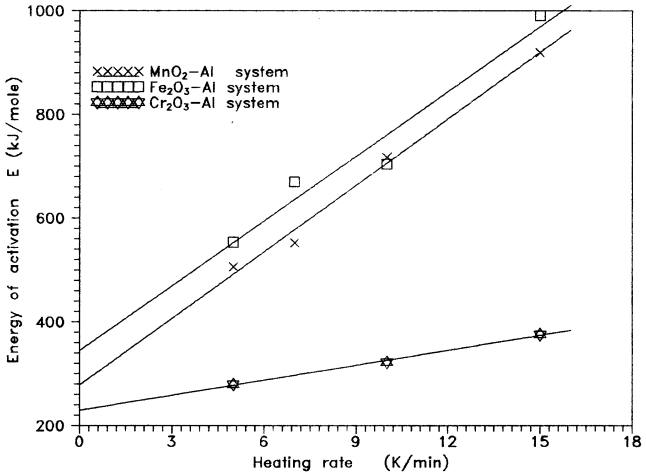

Fig. 2—Plots of activation energy E *vs* heating rate β for Dixit and Ray model.[6]

is not possible to obtain the isothermal oxidation energy value by other methods.

(1) Aluminothermic reductions of Fe_2O_3, MnO_2, and Cr_2O_3 are highly exothermic and fast processes. Prediction of their isothermal reduction kinetics by conventional methods is almost impossible.
(2) Extrapolation of nonisothermal kinetics data provides a unique method for obtaining isothermal kinetics parameters.
(3) Isothermal activation energy values obtained through extrapolation methods are smaller in comparison to nonisothermal values.
(4) Kinetic data obtained using Coats and Redfern[5] and Dixit and Ray[6] approaches compare favorably.

REFERENCES

1. B. Sarangi, H.S. Ray, S. Misra, and A. Sarangi: *Trans. Ind. Inst. Met.*, 1991, vol. 44 (3), p. 279.
2. B. Sarangi, A. Sarangi, and H.S. Ray: *Iron Steel Inst. Jpn. Int.*, 1996, vol. 36 (9), p. 1135.
3. H.S. Ray, B. Sarangi, and A. Sarangi: *Scand. J. Metall.*, 1997, in press.
4. B. Sarangi, H.S. Ray, K.K. Tripathy, and A. Sarangi: *J. Thermal Analysis*, 1994, vol. 44, p. 441.
5. A.W. Coats and J.P. Redfern: *Nature*, 1964, vol. 68, p. 201.
6. S.K. Dixit and H.S. Ray: *Thermochim. Acta*, 1982, vol. 54, p. 245.

Reduction of $FeWO_4$-$NiWO_4$ Solid Solutions by Hydrogen Gas

J.A. BUSTNES, DU SICHEN, and S. SEETHARAMAN

Preparation of heavy alloys is generally started with the blending of metal powders or coreduction of metal oxides.[1] With a view to investigating the coreduction route, a series of reduction studies involving hydrogen gas has been carried out in this laboratory. This includes the reductions of tungsten oxides[2] and some transition metal tungstates, namely, nickel tungstate,[3] cobalt tungstate,[4] and iron tungstate.[5] As a continuation of the previous investigations, the present work aims at a study of the reduction of $NiWO_4$-$FeWO_4$ solid solutions, (Ni, Fe)WO_4, by hydrogen.

(Ni, Fe)WO_4 solid solutions were prepared by mixing nickel tungstate powder (99 pct purity) and iron tungstate powder (99 pct purity), both supplied by Johnson Matthey, Germany in appropriate proportions thoroughly. The powder mixtures were pressed into pellets (about 14 mm in diameter and 5 mm in height) and sintered in a platinum-lined alumina crucible under argon atmosphere (99.9990 pct pure, AGA Gas, Stockholm) at 1473 K for 7 days. X-ray diffraction analyses of the samples carried out in a PHILIPS* X-ray diffraction instrument, ''X-pert system,'' showed the absence of pure $NiWO_4$ and $FeWO_4$, indicating thereby that the two tungstates had reacted completely forming solid solutions. Based on the X-ray diffraction measurements, the lattice parameter values for the two solid solutions as well as the two pure tungstates were evaluated. Figure 1 shows the lattice parameter as a function of composition of the solid solution. The linearity of the variation of lattice parameter with composition suggests that the $NiWO_4$-$FeWO_4$ system follows Vegard's law, which further verifies the formation of the solid solutions.

*PHILIPS is a trademark of Philips Electronic Instruments Corp., Mahwah, NJ.

The thermogravimetric studies were carried out using a SETARAM TGA 92 unit (Setaram, Saint-Cloud, France) with a detection limit of 1 μg. The apparatus and experimental procedure have been described in detail in earlier publications.[2,3] In a general run, the prepared pellet was first ground into fine powder with an average particle size of about 20 μm. About 20 mg powder sample was used. A constant hydrogen flow of 0.52 L·min^{-1} was maintained during the reduction. This flow rate was found, in preliminary experiments, to be beyond the starvation conditions.

In order to identify the phases present in the reduction products, some samples in the form of loosely compacted

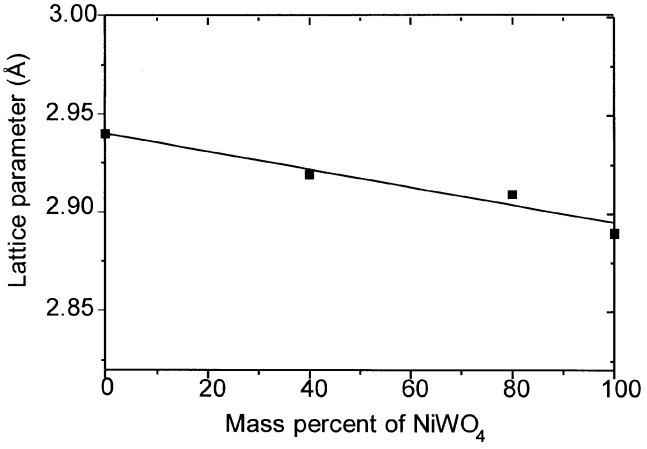

Fig. 1—Lattice parameter as a function of composition of the solid solution.

J.A. BUSTNES, formerly Technical Lic. with the Department of Metallurgy, Royal Institute of Technology, is now Research Metallurgist with LKAB, S-983 81 Malmberget, Sweden. DU SICHEN, Associate Professor, and S. SEETHARAMAN, Professor, are with the Department of Metallurgy, Royal Institute of Technology, S-100 44 Stockholm, Sweden.

Manuscript submitted March 9, 1998.

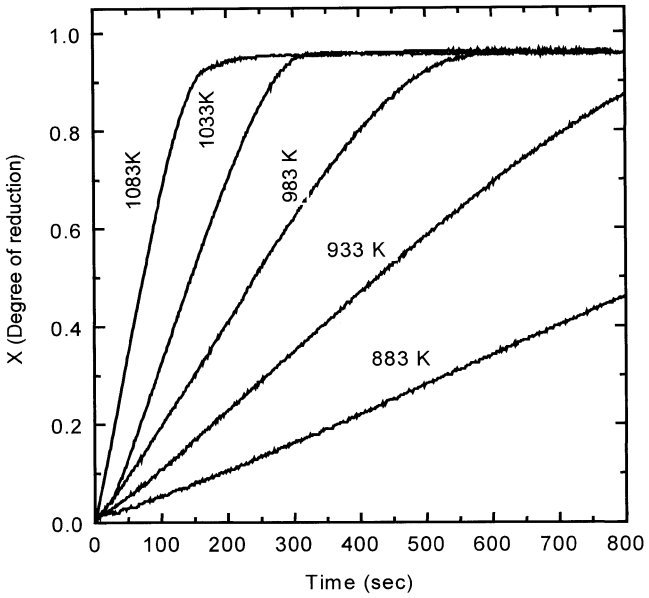

Fig. 2—Reduction curves of the solid solution containing 40 mass pct $NiWO_4$-60 mass pct $FeWO_4$.

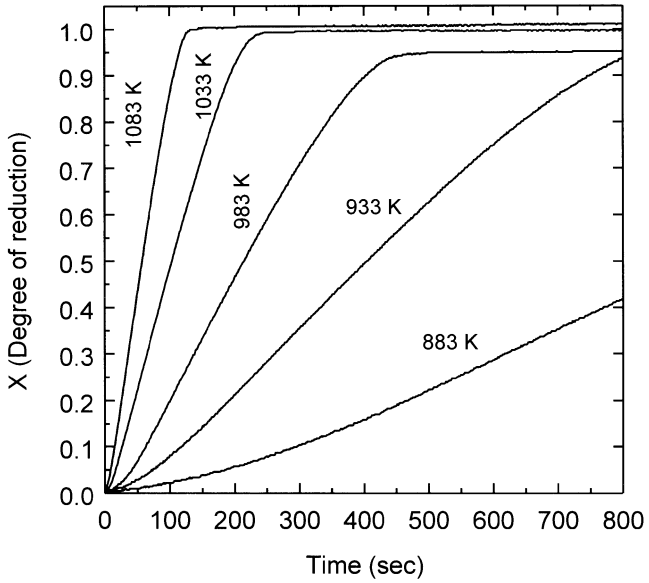

Fig. 3—Reduction curves of the solid solution containing 80 mass pct $NiWO_4$-20 mass pct $FeWO_4$.

pellet were reduced. The reduced pellets were subjected to scanning electron microscope (SEM) analysis. An SEM, model JEOL* JSM-840, connected with electron dispersion spectroscopy (EDS) detector, Link AN-10000, was employed to study the microstructures of the samples and the chemical composition of the phases present.

*JEOL is a trademark of Japan Electon Optics Ltd., Tokyo.

Two (Ni, Fe)WO_4 solid solutions, namely, 40 mass pct $NiWO_4$-60 mass pct $FeWO_4$ and 80 mass pct. $NiWO_4$-20 mass pct $FeWO_4$, were studied in the temperature range of 883 to 1083 K. The reduction curves of these solid solutions are presented in Figures 2 and 3, respectively. The dimensionless mass change, X, represents the ratio of the instant mass loss, ΔW_t, to the theoretical final mass loss, ΔW_∞, the latter corresponding to the loss of all four oxygen atoms from (Ni, Fe)WO_4. It is seen that the reductions proceed fast. Even at 883 K, the reductions of the samples reach a value of $X > 0.4$ after 800 seconds. The reaction rates increase considerably with temperature in the case of both solid solutions. At 1083 K, the reductions of the samples all finish within 150 seconds.

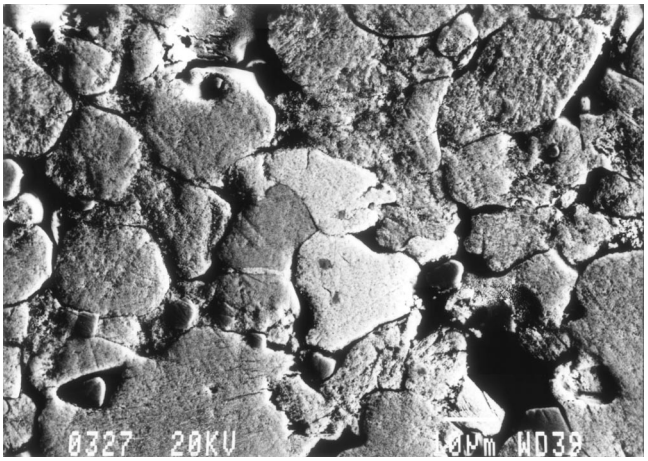

Fig. 4—Photomicrograph of the reduced solid solution containing 40 mass pct $NiWO_4$-60 mass pct $FeWO_4$.

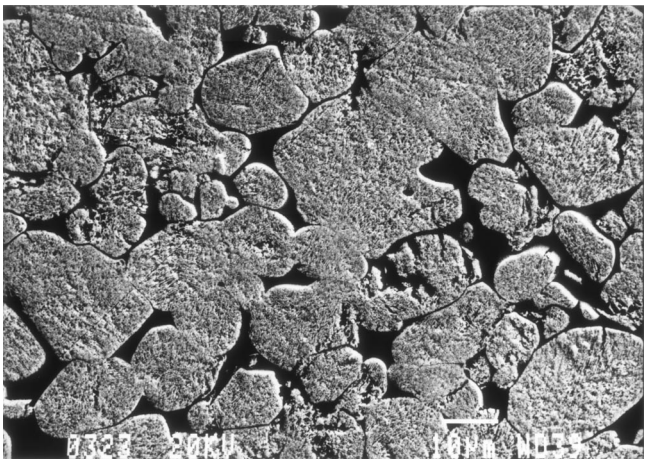

Fig. 5—Photomicrograph of the reduced solid solution containing 80 mass pct $NiWO_4$-20 mass pct $FeWO_4$.

Figures 4 and 5 present the photomicrographs of the 40 mass pct $NiWO_4$-60 mass pct $FeWO_4$ and 80 mass pct $NiWO_4$-20 mass pct $FeWO_4$ samples reduced at 1033 K. It is seen in Figure 4 that three phases could be identified in the reduced sample of 40 mass pct $NiWO_4$-60 mass pct $FeWO_4$ solution. According to the EDS analyses, the white phase is tungsten, the slightly darker phase is Fe-Ni-W solid solution rich in tungsten and iron, and the darkest phase is a Fe-Ni-W solid solution rich in nickel. The microstructures in the reduced samples of 80 mass pct $NiWO_4$-20 mass pct $FeWO_4$ are not clear. While the photomicrograph shown in Figure 5 appears to suggest a uniform structure with two phases, one white and one darker finely mixed, attempts by EDS analysis to identify the phases were not successful.

In order to understand the reduction mechanisms from a thermodynamic viewpoint, the phase diagram[6] of the Fe-Ni-W ternary system at 1073 K is reproduced in Figure 6.

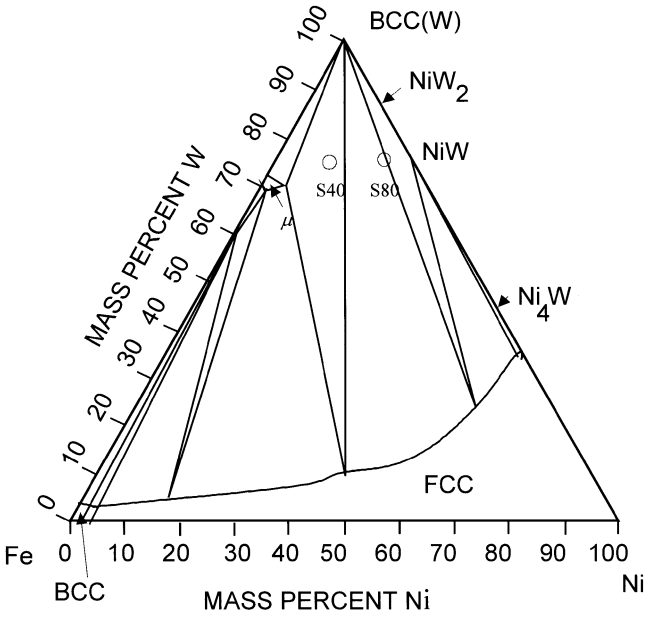

Fig. 6—Phase diagram of the Fe-Ni-W system at 1023 K.

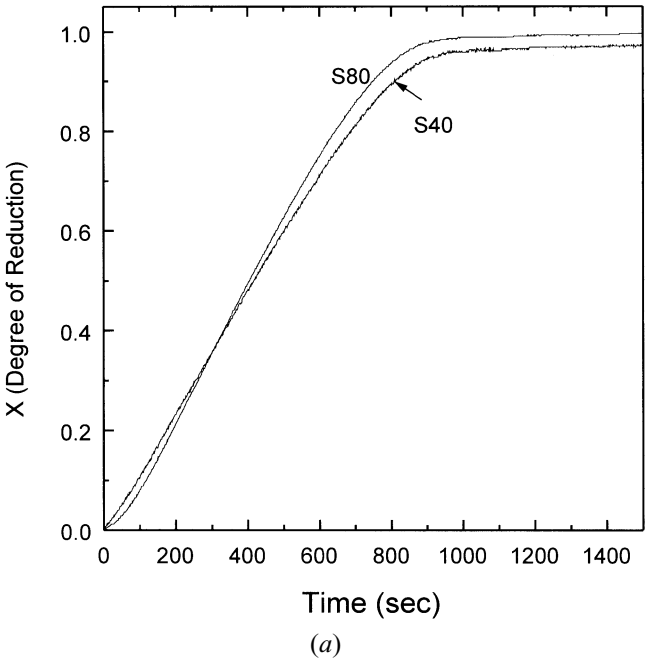

(*a*)

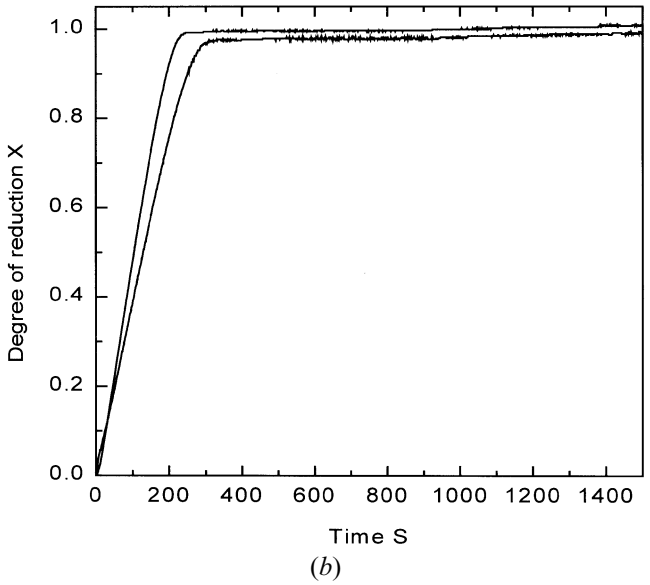

(*b*)

Fig. 7—(*a*) Comparison of the reductions of the two solid solutions carried out at 933 K (S40: 40 mass pct $NiWO_4$-60 mass pct $FeWO_4$, and S80: 80 mass pct $NiWO_4$-20 mass pct $FeWO_4$). (*b*) Comparison of the reductions of the two solid solutions carried out at 1033 K (S40: 40 mass pct $NiWO_4$-60 mass pct $FeWO_4$, S80: 80 mass pct $NiWO_4$-20 mass pct $FeWO_4$).

The average compositions of the reduction products of the two solid solutions are also presented in the same figure, with S40 and S80 denoting the solution of 40 mass pct $NiWO_4$-60 mass pct $FeWO_4$ and 80 mass pct $NiWO_4$-20 mass pct $FeWO_4$ respectively. It is seen that while the composition of the reduced S40 solution falls in the bcc(W)-fcc-μ three-phase region, the composition of the reduced S80 solution belongs to the bcc(W)-fcc two-phase area. The results of the EDS analyses in the S40 solution are in accordance with the phase diagram. As mentioned previously three phases were identified in the reduced sample. The slightly white phase in Figure 4 is the bcc(W) phase. The darker phase, rich in W and Fe, and the darkest phase, rich in Ni, are μ phase and fcc solid solution, respectively. As the reduction curves indicate a single step, it is reasonable to conclude that S40 solution is reduced by hydrogen directly to a three-phase mixture, *viz*. bcc-fcc-μ. On the other hand, the result of the EDS analysis in the reduced S80 sample was not conclusive. It is seen in Figure 5 that hydrogen reduction of this sample results in a uniform and very fine structure. Although the photomicrograph appears to suggest that there are two phases, a white and a slightly darker, mixing very well together, no conclusion can be made regarding the compositions of these phases. It was impossible to make any EDS analysis due to the fine grains of the two phases. However, the phase diagram shown in Figure 6 indicates that the sample after reduction should consist of two phases, namely, bcc and fcc. This phase relationship seems to be in accordance with the microstructure in the reduced S80 sample.

The absence of a break point in the reduction curves in Figures 2 and 3 suggests that there was no change in reaction mechanism during each individual reduction. Since both reductions in S40 and S80 proceed in a single step, the reactions can be expressed by the following equation:

$$\frac{1}{4}\,(\text{Fe, Ni})WO_4 + H_2\,(\text{gas}) = \text{Alloy} + H_2O\,(\text{gas}) \qquad (1)$$

It is noted that ''Alloy'' on the right-hand side of Eq. [1] stands for different phase mixtures when different (Fe, Ni)WO_4 solutions are studied. In the case of S40, ''Alloy'' represents a bcc(W)-fcc-μ mixture, whereas ''Alloy'' denotes a two-phase mixture bcc(W)-fcc in the reduction of S80.

In view of the different reduction products of S40 and S80, it would be interesting to compare the reduction curves of the two solid solutions. In Figures 7(a) and (b), the comparisons are made for the reductions carried out at 933 and 1033 K, respectively. It is seen that the reduction curves obtained for these two solutions are very similar. Irrespective of the temperature, the reduction rates of the two solutions show only a slight difference. That the S40 shows a higher initial reduction rate in both cases could

well be within the experimental uncertainties. The similarity of the reduction curves shown in both Figures 7(a) and (b) would suggest that the breakdown of the chemical bonds in the two tungstate solid solutions by hydrogen might take place in the same manner, although the reduction products are different.

It was found by one of the present authors[5] that the reduction of pure $FeWO_4$ by H_2 also took place in a single step, the product being a mixture of tungsten and the μ phase. On the other hand, $NiWO_4$ is reduced by hydrogen in two steps.[3] The reduction starts with the breakdown of the Ni-O bonding resulting in Ni and WO_2 as the first stage. This is followed by the reduction of WO_2 to W. The reductions of the solid solutions are in line with the one step trend but differ from the reduction of pure $NiWO_4$. In the case of nickel tungstate, the bonding between Ni and O is weaker than that of W-O. The Ni-O bondings will be broken first, resulting in the loss of two oxygen atoms in connection with Ni, before the breakdown of the rest of the W-O bondings. In the case of the solid solutions, if the two tungstates mix ideally, the two metal cations, Ni^{2+} and Fe^{2+}, are expected to be randomly distributed in the tungstate matrix, where oxygen ions are strongly linked to the W^{6+} ions. The linear change of the molar volume, as indicated by Figure 1, seems to support the hypothesis of ideal mixing of the solid solution. The stabilization of $NiWO_4$ due to the decrease of thermodynamic activity would offer certain resistance to the differential reduction of $NiWO_4$ in two steps.

It was mentioned in the experimental discussion that very small (20 mg) powder samples in the form of a shallow bed were employed. As the particle size of the sample was very small and the hydrogen flow rate was high, the reduction could be expected to be controlled by the chemical reaction at the initial stages of the reduction. It is possible to evaluate the activation energies for the reductions of the two solid solutions using the initial reaction rates at different temperatures. It is noted that a few seconds would be required for the reaction chamber to attain a hydrogen pressure of 1 atm due to the gas switch. Hence, the initial reaction rate was taken at the moment when the reaction rate showed a maximum. While the Arrhenius plot for S40 yields an activation energy of 90 kJ·mole, the Arrhenius plot for S80 results in an activation energy value of 97 kJ·mole. These two values are compared with the activation energies for the hydrogen reduction of $NiWO_4$[3] and $FeWO_4$[5] in Figure 8. The value of $NiWO_4$ in this figure corresponds to the reduction of this compound to Ni and WO_2. The activation energies appear to follow a trend that higher nickel content in the solution would lead to higher activation energy value.

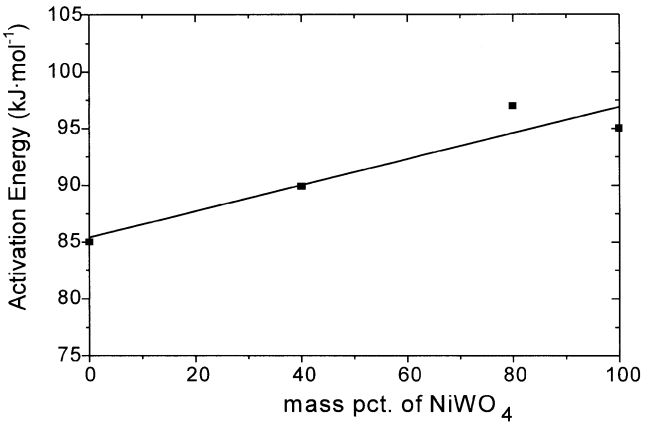

Fig. 8—Activation energy as a function of the composition of solid solution.

It is worthwhile to mention that the reductions of the two tungstate solutions result in very different microstructures, despite the similarities in the reduction curves. This aspect could have an important impact on the heavy metal industry. It could be possible to predict the morphology of a product by choosing a suitable oxide mixture for coreduction. For example, the S80 solution would yield a uniformly distributed bcc-fcc two-phase mixture, as shown in Figure 4. The fine structure and homogeneity of the reduction product would be useful in the production of heavy meals with desired mechanical properties.

REFERENCES

1. S.W.H. Yih and C.T. Wang: *Tungsten*, Plenum Press, New York, NY, 1979, pp. 358-62.
2. J.A. Bustnes, Du Sichen, and S. Seetharaman: *Metall. Trans. B*, 1993, vol. 24B, pp. 475-80.
3. S. Sridhar, Du Sichen, and S. Seetharaman: *Metall. Mater. Trans. B*, 1994, vol. 25B, pp. 391-96.
4. J.A. Bustnes, Du Sichen, and S. Seetharaman: *Metall. Mater. Trans. B*, 1995, vol. 26B, pp. 547-52.
5. J.A. Bustnes: *Metall. Mater. Trans. B*, 1997, vol. 28B, pp. 613-18.
6. A.F. Guillermet and L. Östlund: *Metall. Trans. A*, 1986, vol. 17A, pp. 1809-23.